Mantle transition zone thinning beneath eastern Africa: Evidence for a whole-mantle superplume structure

Gabriel D. Mulibo[1,2] and Andrew A. Nyblade[1]

Received 7 May 2013; revised 20 June 2013; accepted 21 June 2013.

[1] *P* to *S* conversions from the 410 and 660 km discontinuities observed in receiver function stacks reveal a mantle transition zone that is ~30–40 km thinner than the global average in a region ~200–400 km wide extending in a SW-NE direction from central Zambia, across Tanzania and into Kenya. The thinning of the transition zone indicates a ~190–300 K thermal anomaly in the same location where seismic tomography models suggest that the lower mantle African superplume structure connects to thermally perturbed upper mantle beneath eastern Africa. This finding provides compelling evidence for the existence of a continuous thermal structure extending from the core-mantle boundary to the surface associated with the African superplume.
Citation: Mulibo, G. D., and A. A. Nyblade (2013), Mantle transition zone thinning beneath eastern Africa: Evidence for a whole-mantle superplume structure, *Geophys. Res. Lett.*, *40*, doi:10.1002/grl.50694.

1. Introduction

[2] Imaging density-driven upwellings that extend from the lower mantle into the upper mantle has remained a challenge ever since the first mantle plume models were proposed more than 40 years ago [*Morgan*, 1971], leading to much debate about the modes and scales of mantle convection. Seismic tomography models show that in some subduction zones, lithospheric slabs penetrate through the mantle transition zone and extend to the core-mantle boundary [*Grand et al*., 1997; *van der Hilst et al*., 1997], forming whole-mantle density-driven downwellings. Comparable seismic evidence for whole-mantle upwellings originating at the core-mantle boundary (CMB), however, is still lacking. It has been suggested often that large thermal and/or chemical upwellings in the lower mantle beneath southern Africa and the southern Pacific ocean (the so-called African and Pacific superplumes) may constitute such upwellings [e.g., *McNamara and Zhong*, 2005; *Garnero and McNamara*, 2008], but imaging the midmantle in these regions is difficult, and therefore, it remains uncertain if those structures extend into the upper mantle [*He and Wen*, 2009; *Schmerr et al*., 2010; *Ritsema et al*., 2007; *Simmons et al*., 2007]. For example, recent seismic tomography images of the African mantle trace the upper surface of the African superplume to depths of 800–1100 km [*Hansen et al*., 2012; *Mulibo and Nyblade*, 2013], while images of upper mantle and transition zone structure beneath eastern Africa trace the lower surface of an upper mantle anomaly to depths of ~500–600 km [*Owens et al*., 2000; *Huerta et al*., 2009; *Adams et al*., 2012; *Mulibo and Nyblade*, 2013], leaving open the possibility that the superplume structure might be separated from anomalous upper mantle structure under eastern Africa by a region of normal mantle that is a few hundred kilometers thick.

[3] Here we present evidence for a thin mantle transition zone beneath eastern Africa, which indicates that a thermal anomaly spans the transition zone and connects the tomographically imaged lower and upper mantle structures. The evidence comes from mapping topography on the 410 and 660 km discontinuities using *P* to *S* conversions observed in receiver functions. The mantle transition zone is bounded by seismic discontinuities that result from mineral phase transformations of olivine to wadsleyite at ~410 km depth, and ringwoodite to Mg-perovskite and magnesiowustite near 660 km depth [*Morishima et al*., 1994; *Katsura et al*., 2004; *Fei et al*., 2004]. Because the Clapeyron slopes are opposite in sign for the 410 and 660 km discontinuities, the depths of the discontinuities, as well as the thickness of the region between them (i.e., the transition zone thickness or TZT), provide information about the thermal structure across the ~400–700 km depth interval in the mantle.

2. Data and Methodology

[4] To improve seismic data coverage in eastern Africa, the AfricaArray eastern African seismic experiment (AAEASE) was launched in 2007. Twenty broadband stations were initially deployed in Uganda and northwestern Tanzania in August 2007 for 18 months (Phase I), and then most of the stations were redeployed in December 2008 across southern Tanzania (Phase II) (Figure 1). In August 2010, the stations were redeployed again in Zambia and operated through July 2011 (Phase III). An affiliated network of stations belonging to the AfricaArray Tanzania basin seismic experiment (AATBSE) was also deployed in southeastern Tanzania from February 2010 to July 2011 (Figure 1). Data recorded by these stations have been combined with data from permanent stations and other temporary networks in the region for this study (Figure 1).

[5] Seismograms used for computing teleseismic *P* wave receiver functions (PRFs) come from earthquakes with $m_b \geq 5.0$ distributed over a wide range of back azimuths and distances between 30°–90° from the stations (Figure S1a in the supporting information). An iterative time-domain deconvolution method was used to compute the receiver

Additional supporting information may be found in the online version of this article.

[1]Department of Geosciences, Pennsylvania State University, University Park, Pennsylvania, USA.
[2]School of Earth Sciences and Engineering, Nelson Mandela African Institute of Science and Technology, Arusha, Tanzania.

Corresponding author: G. D. Mulibo, Department of Geosciences, Pennsylvania State University, 402 Deike Bldg., University Park, PA 16802, USA. (gdm135@psu.edu)

©2013. American Geophysical Union. All Rights Reserved.
0094-8276/13/10.1002/grl.50694

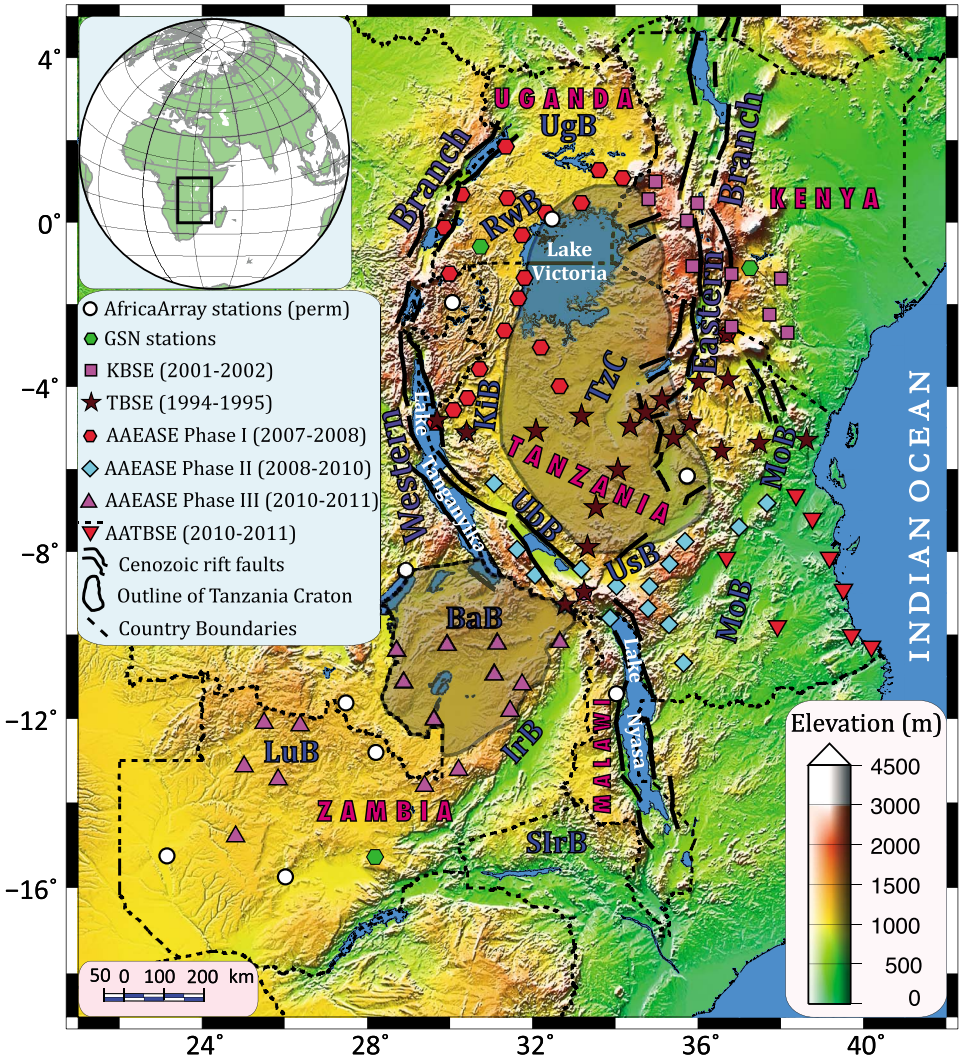


Figure 1. Topographic map showing the geology of eastern Africa and the locations of seismic stations. The Precambrian tectonic framework is comprised of the Archean Tanzania Craton (TzC), which likely includes the Uganda Basement Complex (UgB), the Bangweulu Block (BaB), and several Proterozoic mobile belts (Rwenzori, RwB; Kibaran, KiB; Ubendian, UbB; Usagaran, UsB; Mozambique, MoB; Iruminde, IrB; Southern Iruminde, SIrB; Lufilian, LuB). The inset map shows the location of the study area. GSN, Global Seismograph Network. KBSE, Kenya Broadband Seismic Network [*Nyblade and Langston*, 2002]. TBSE, Tanzania Broadband Seismograph Network [*Nyblade et al*., 1996].

functions from vertical, radial, and transverse component seismograms [*Ligorría and Ammon*, 1999]. The PRFs were quantitatively evaluated using a least squares misfit criterion for assessing the percentage recovered from the original radial component. The misfit criterion is computed from the difference between the radial component seismogram and the convolution of the vertical component seismogram with the already determined radial receiver function. A misfit of 85% was used as the threshold in selecting the PRFs that were considered for further processing. Also, events with large-amplitude tangential receiver functions were not used, even if they passed the 85% threshold.

[6] Receiver functions were stacked using a geographical binning technique described by *Owens et al*. [2000] and a 3-D mantle velocity model from *Mulibo and Nyblade* [2013]. Crustal structure in the 3-D model was replaced with the crustal structure from *Last et al*. [1997]. To obtain a good signal-to-noise ratio in the receiver function stacks, several parameters were tested, including computing PRFs for a range of Gaussian filter widths, adjusting the stacking bin radius from 1.0° to 1.5°, changing the minimum number of receiver functions in each stack from 7 to 40, varying the minimum number of stations within a stacking bin from 3 to 4, and using the 1-D IASP91 model [*Kennett and Engdahl*, 1991], in addition to the 3-D velocity model. Through testing various combinations of parameters, we found that the optimal parameters yielding clear P410s and P660s arrivals included the 3-D velocity model, a minimum of 30 receiver functions per bin from at least three stations, a bin radius of 1.0°, a bin increment of 0.25°, and a Gaussian filter width of 0.5 (frequency of 0.24 Hz). The 3-D velocity model, in particular, greatly improved the quality of the stacks (Figures S2a and S2b).

[7] Bootstrapped error analysis applied to a subset of the data by *Owens et al*. [2000] for a fixed velocity model yielded a depth resolution of ±3 km. However, taking into account the uncertainties in crustal thickness [*Last et al*., 1997] and upper mantle velocities [*Mulibo and Nyblade*, 2013], we

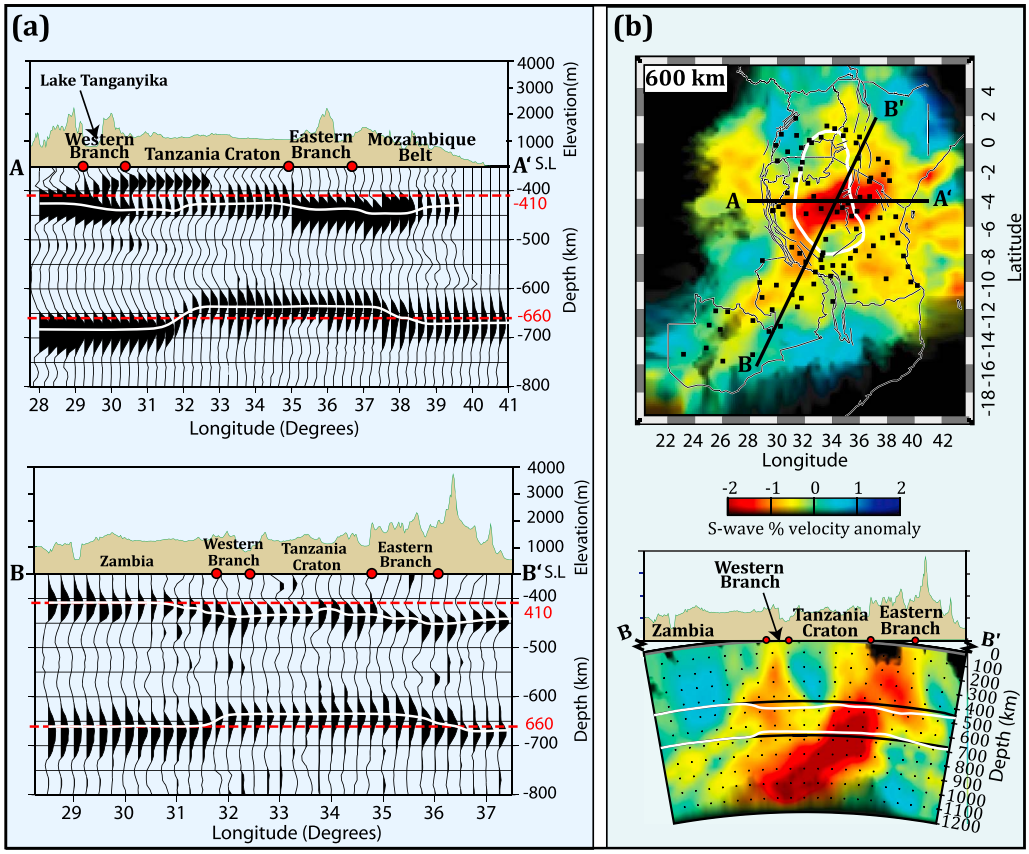


Figure 2. (a) Profiles of receiver function stacks displaying *P*-to-*S* conversions from the 410 and 660 km discontinuities. Profile locations are shown in Figure 2b. The solid white lines show the picked depths of the 410 and 660 km discontinuities. (b) *S* wave speed images from *Mulibo and Nyblade* [2013] at 600 km depth and vertically along profile B–B′. Small black squares show station locations.

estimate the uncertainty in the discontinuity depths to be between 5 and 10 km, similar to the uncertainties reported by *Owens et al*. [2000] and *Huerta et al*. [2009].

3. Results

[8] The location of *P*-to-*S* conversion points at 410 and 660 km depth provides good spatial coverage over most of eastern Africa (Figures S1b and S1c), including all of the major Precambrian terrains that form the basement structure of the region, plus the Eastern and Western branches of the Cenozoic East African rift system (Figure 1). Receiver function stacks are illustrated in Figure 2a for two profiles, one crossing the East African Plateau from east to west (A–A′) and the other from southwest to northeast (B–B′). In profile A–A′, P410s arrivals beneath the Western branch can be seen at a depth of 430–440 km; they shallow by about 10 km beneath the Tanzania Craton in the middle of the profile and then deepen again beneath the Eastern branch and the Mozambique Belt. The P660s arrivals beneath the Western branch are visible at a depth of 670–680 km, shallow to ~650 km depth in the portion of the profile beneath the Craton and the Eastern branch and then deepen to a depth of ~660–670 km beneath the Mozambique Belt.

[9] Significant variation in the depths of the 410 and 660 km discontinuities can also be seen in profile B–B′ (Figure 2a), which stretches southwest to northeast from central Zambia to northern Kenya, crossing the Western branch, the Tanzania Craton, and the Eastern branch. Beneath Zambia, the P410s arrivals are visible at a depth of 410 km and shift deeper to 430–440 km beneath the Western branch. Beneath the Tanzania Craton, the P410s arrivals are visible at a depth of 420–430 km and deepen beneath the Eastern rift to a depth of 440–450 km. For the 660 km discontinuity, the P660s arrivals are visible at a depth of 660 km beneath Zambia, are shallower (~650–640 km depth) in the portion of the profile beneath the Western branch, the Tanzania Craton, and the Eastern branch, and are visible at a depth of ~660–670 km along the northeastern end of the profile.

4. Discussion

[10] Variations in the depths of the 410 and 660 km discontinuities across the region show a strong correlation with the location of the low wave speed anomaly in the 3-D tomography model (Figures 2b and S3) [*Mulibo and Nyblade*, 2013], providing clear evidence for a thermal anomaly extending across the transition zone. Previous studies of the discontinuities and upper mantle velocity structure in eastern Africa [*Owens et al*., 2000; *Huerta et al*., 2009] showed a depressed 410 km discontinuity beneath the Eastern branch of the rift system, indicating that the thermally perturbed structure in the upper mantle extends across the 410 km discontinuity and into the transition zone. The 660 km discontinuity was imaged at depths of ~680–690 km in those studies and was flat. We attribute the difference between that result and our

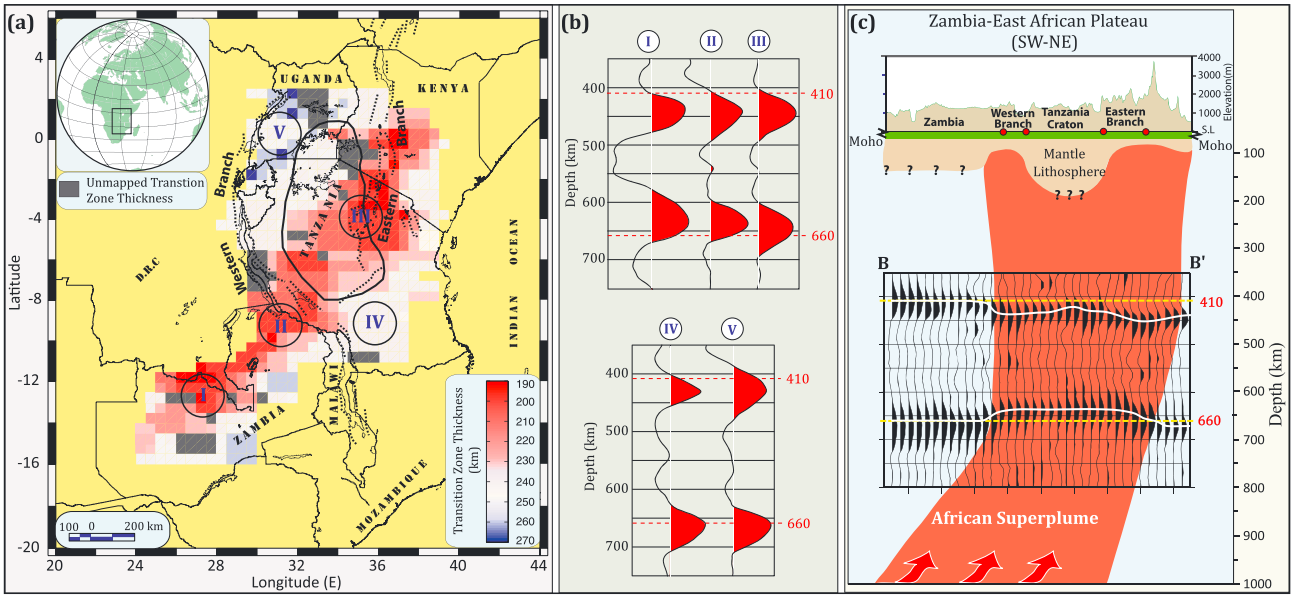


Figure 3. Transition zone thickness, receiver function stacks, and cartoon of mantle upwelling. (a) Map showing the TZT across the study region. The gray regions show areas where the TZT could not be determined. The bold black line shows the outline of the Tanzania Craton and the dashed lines show major Cenozoic rift faults. (b) Receiver function stacks for 1.5° radius bins. Bin locations are shown in Figure 3a. (c) Schematic cross section for profile B–B′ showing upwelling of the African superplume through the mantle transition zone. The receiver function stacks showing that the 410 and 660 km discontinuities are superimposed, with the white line indicating the picked depths.

images of the 660 km discontinuity mostly to the improved depth migration of the receiver function stacks using the 3-D velocity model of *Mulibo and Nyblade* [2013], which has better resolution, especially in the transition zone, than the 3-D model of *Ritsema et al.* [1998] used by *Owens et al.* [2000] and the 1-D IASP91 model used by *Huerta et al.* [2009].

[11] Because both the P410s and P660s arrivals can be similarly affected by velocity structure above the transition zone that might not be fully resolved in the 3-D velocity model [*Mulibo and Nyblade*, 2013], the TZT provides a better estimate of the temperature anomaly spanning the transition zone than do the depths of the discontinuities themselves. A map of the TZT (Figure 3a) shows a region trending from the southwest (Zambia) to the northeast (Kenya) that is ~200–400 km wide with an average TZT of 210 km. This is in contrast to a TZT in southeastern Tanzania of 240–250 km, and a TZT in northwestern Tanzania, and eastern and southern Zambia of 250–260 km. A TZT of 210 km is ~30–40 km thinner than the global average estimates for the TZT of 242–250 km [*Flanagan and Shearer*, 1998; *Chevrot et al.*, 1999; *Lawrence and Shearer*, 2006], while the TZT of 240–260 km beneath the other regions is in closer agreement with the global average estimates. Receiver function stacks incorporating data from larger areas in each one of these regions further illustrate the thinning of the transition zone in a SW-NE swath across Zambia, Tanzania, and Kenya (Figures 3b and S2b).

[12] The temperature perturbation across the transition zone can be estimated using a Clapeyron slope of 3.6 to 4.0 MPa K^{-1} for the 410 km discontinuity and −1.0 to −2.0 MPa K^{-1} for the 660 km discontinuity [*Morishima et al.*, 1994; *Katsura et al.*, 2004; *Fei et al.*, 2004]. Thirty to 40 km of transition zone thinning in the SW-NE swath beneath Zambia, Tanzania, and Kenya yields a thermal anomaly of ~190–300 K. A thermal anomaly of this magnitude is consistent with the velocity model used for the 3-D migration of the receiver functions showing reductions in *S* wave speeds, coincident with the location of the thinned transition zone. It is also consistent with estimates of thermal anomalies in the upper mantle obtained from seismic attenuation (280 K) [*Venkataraman et al.*, 2004] and petrologic studies (~140–170 K) [*Rooney et al.*, 2012].

[13] A 190–300 K thermal anomaly spanning the transition zone exactly where the seismic images suggest anomalies in the lower and upper mantle connect [e.g., *Hansen et al.*, 2012; *Simmons et al.*, 2012; *Mulibo and Nyblade*, 2013] provides compelling evidence for a throughgoing mantle thermal structure associated with the African superplume. The thermal structure, which is centered under southern Africa in the lowermost mantle and tilts to the northeast as it rises toward the upper mantle (Figure 3c), represents an upwelling mode of whole-mantle convection that is on the same vertical scale as the downwelling mode of whole-mantle convection represented by sinking lithospheric slabs.

[14] Although a throughgoing mantle thermal structure is associated with the superplume, many questions about the superplume remain. For example, how does compositional heterogeneity affect the density-driven flow? Where does the excess heat and/or anomalous chemistry within the structure come from? Why does the structure tilt toward the northeast in the midmantle? And is there mantle flow across the 660 km discontinuity? If the 660 km discontinuity creates a barrier to the rising superplume material in the lower mantle [*Davies*, 1995], then warm superplume material ponding beneath the 660 km discontinuity could heat the bottom of the transition zone, generating secondary thermal plumes that rise from within the transition zone toward the surface [e.g., *Yuen et al.*, 2007; *Farnetani and Hofmann*, 2009]. Helium isotopic evidence suggests that there could be some flux of

lower mantle material across the 660 km discontinuity [*Pik et al*., 2006; *Hilton et al*., 2011], as do some radiogenic isotopic data [*Rooney et al*., 2012].

5. Conclusions

[15] The average transition zone thickness in a region ~200–400 km wide beneath Zambia, Tanzania, and Kenya is 210 ± 10 km, indicating the presence of an ~190–300 K thermal anomaly spanning the transition zone under eastern Africa. The location of the thermal anomaly coincides with the region where seismic tomography images show the lower mantle African superplume anomaly connecting with anomalous upper mantle structure under eastern Africa. This result provides clear evidence that the superplume is a whole-mantle structure composed of at least a thermal anomaly extending from the core-mantle boundary to the surface.

[16] **Acknowledgments.** This study was funded by the National Science Foundation (grants OISE-0530062, EAR-0440032, EAR-0824781). We gratefully acknowledge IRIS-PASSCAL, the Tanzania Geological Survey, the University of Dar es Salaam, the Uganda Geological Survey, the Zambia Geological Survey, Penn State University, and many individuals from those institutions for assistance with fieldwork. We also thank two anonymous reviewers for constructive comments that improved the paper.

[17] The Editor thanks two anonymous reviewers for their assistance in evaluating this paper.

References

Adams, A., A. A. Nyblade, and D. Weeraratne (2012), Upper mantle shear wave velocity structure beneath the east African plateau: Evidence for a deep, plateauwide low velocity anomaly, *Geophys. J. Int.*, *189*(1), 123–142.

Chevrot, S., L. Vinnik, and J.-P. Montagner (1999), Global-scale analysis of the mantle *Pds* phases, *J. Geophys. Res.*, *104*, 20203–20219.

Davies, G. F. (1995), Penetration of plates and plumes through the mantle transition zone, *Earth Planet. Sci. Lett.*, *133*, 507–516.

Farnetani, C. G., and A. W. Hofmann (2009), Dynamics and internal structure of a lower mantle plume conduit, *Earth Planet. Sci. Lett.*, *282*, 314–322.

Fei, Y., J. Van Orman, J. Li, W. van Westrenen, C. Sanloup, W. Minarik, K. Hirose, T. Komabayashi, M. Walter, and K. Funakoshi (2004), Experimentally determined postspinel transformation boundary in Mg_2SiO_4 using MgO as an internal pressure standard and its geophysical implications, *J. Geophys. Res.*, *109*, B02305, doi:10.1029/2003JB002562.

Flanagan, M. P., and P. M. Shearer (1998), Global mapping of topography on transition zone velocity discontinuities by stacking SS precursors, *J. Geophys. Res.*, *103*, 2673–2692.

Garnero, E. J., and A. K. McNamara (2008), Structure and dynamics of Earth's lower mantle, *Science*, *320*, 626–628, doi:10.1126/science.1148028.

Grand, S. P., R. D. van der Hilst, and S. Widitantoro (1997), Global seismic tomography: A snapshot of convection in the Earth, *GSA Today*, *7*, 1–7.

Hansen, S., A. A. Nyblade, and M. Benoit (2012), Mantle structure beneath Africa and Arabia from adaptively parameterized *P*-wave tomography: Implications for the origin of Cenozoic Afro-Arabian tectonism, *Earth Planet. Sci. Lett.*, *319–320*, 23–34.

He, Y., and L. Wen (2009), Structural features and shear-velocity structure of the "Pacific Anomaly", *J. Geophys. Res.*, *114*, B02309, doi:10.1029/2008JB005814.

van der Hilst, R. D., S. Widyantoro, and E. R. Engdahl (1997), Evidence for deep mantle circulation from global tomography, *Nature*, *386*, 578–584.

Hilton, D. R., S. A. Halldorsson, P. H. Barry, T. P. Fischer, J. M. de Moor, C. J. Ramirez, F. Mangasini, and P. Scarsim (2011), Helium isotopes at Rungwe Volcanic Province, Tanzania, and the origin of East African Plateaux, *Geophys. Res. Lett.*, *38*, L21304, doi:10.1029/2011gl049589.

Huerta, A., A. A. Nyblade, and A. Reusch (2009), Mantle transition zone beneath Kenya and Tanzania: More evidence for deep-seated thermal upwelling in the mantle, *Geophys. J. Int.*, *177*, 1249–1255.

Katsura, T., et al. (2004), Olivine-wadsleyite transition in the system (Mg,Fe)$_2SiO_4$, *J. Geophys. Res.*, *109*(B2), B02209, doi:10.1029/2003JB002438.

Kennett, B. L. N., and E. R. Engdahl (1991), Traveltimes for global earthquake location and phase identification, *Geophys. J. Int.*, *105*(2), 429–465, doi:10.1111/j.1365-246X.1991.tb06724.x.

Last, R. J., A. A. Nyblade, C. A. Langston, and T. Owens (1997), Crustal structure of the East African Plateau from receiver functions and Rayleigh wave phase velocities, *J. Geophys. Res.*, *102*, 24469–24483.

Lawrence, J. F., and P. M. Shearer (2006), A global study of transition zone thickness using receiver functions, *J. Geophys. Res.*, *111*, B06307, doi:10.1029/2005JB003973.

Ligorría, J. P., and C. J. Ammon (1999), Iterative deconvolution and receiver function estimation, *Bull. Seismol. Soc. Am.*, *89*, 1395–1400.

McNamara, A. K., and S. Zhong (2005), Thermochemical piles under Africa and the Pacific, *Nature*, *437*, 1136–1139, doi:10.1038/nature04066.

Morgan, W. J. (1971), Convection plumes in the lower mantle, *Nature*, *230*, 42–3.

Morishima, H., T. Kato, M. Suto, E. Ohtani, S. Urakawa, W. Utsumi, O. Shimomura, and T. Kikegawa (1994), The phase boundary between α- and β-Mg_2SiO_4 determined by in situ X-ray observation, *Science*, *265*, 1202–1203.

Mulibo G. D., and A. A. Nyblade (2013), The *P* and *S* wave velocity structure of the mantle beneath eastern Africa and the African superplume anomaly, *Geochem. Geophys. Geosyst.*, doi:101002/ggge.20150.

Nyblade, A. A., and C. Langston (2002), Broadband seismic experiments probe the East African rift, *Eos. Trans. AGU*, *83*(405), 408–409.

Nyblade, A. A., C. Birt, C. Langston, T. Owens, and R. Last (1996), Seismic experiments reveals rifting of craton in Tanzania, *Eos. Trans. AGU*, *77*, 517–521.

Owens, T., A. A. Nyblade, H. Gurrola, and C. Langston (2000), Mantle transition zone structure beneath Tanzania, East Africa, *Geophys. Res. Lett.*, *27*(6), 827–830.

Pik, R., B. Marty, and D. R. Hilton (2006), How many mantle plumes in Africa? The geochemical point of view, *Chem. Geol.*, *226*, 100–114.

Ritsema, J., A. A. Nyblade, T. J. Owens, C. A. Langston, and J. C. VanDecar (1998), Upper mantle seismic velocity structure beneath Tanzania, East Africa: Implications for the stability of cratonic lithosphere, *J. Geophys. Res.*, *103*, 21201–21213.

Ritsema, J., A. K. McNamara, and A. L. Bull (2007), Tomographic filtering of geodynamic models: Implications for model interpretation and large-scale mantle structure, *J. Geophys. Res.*, *112*, B01303, doi:10.1029/2006JB004566.

Rooney, T., C. Herzberg, and I. Bastow (2012), Elevated mantle temperature beneath East Africa, *Geology*, *40*(G32382R1), 27–40, doi:10.1130/G32382.1.

Schmerr, N., E. Garnero, and A. McNamara (2010), Deep mantle plumes and convective upwelling beneath the Pacific Ocean, *Earth Planet. Sci. Lett.*, *294*, 143–151.

Simmons, N. A., A. M. Forte, and S. P. Grand, (2007), Thermochemical structure and dynamics of the African superplume, *Geophys. Res. Lett.*, *34*, L02301, doi:10.1029/2006GL028009.

Simmons, N. A., S. C. Myers, G. Johannesson, and E. Matzel (2012), LLNL-G3Dv3: Global P wave tomography model for improved regional and teleseismic travel time prediction, *J. Geophys. Res.*, *117*, B10302, doi:10.1029/2012JB009525.

Venkataraman, A., A. A. Nyblade, and J. Ritsema (2004), Upper mantle Q and thermal structure beneath Tanzania, East Africa, from teleseismic *P*-wave spectra, *Geophys. Res. Lett.*, *31*(4), L15611, doi:10.1029/2004GL020351.

Yuen, D. A., M. Monnereau, U. Hansen, M. Kameyama, and C. Matyska (2007), Dynamics of superplumes in the lower mantle, in *Superplumes: Beyond Plate Tectonics*, edited by D. A. Yuen, S. Maruyama, S. Karato, and B. F. Windley, 239–268 pp., Springer Verlag, Heidelberg.